Measurement of the CP violation in $B_s^0 \to J/\psi\phi$ decays in p-p collisions at $\sqrt{s}$ = 13 TeV with the ATLAS detector

Maria Smizanska
on behalf of the ATLAS collaboration

Lancaster University

DISCRETE 2021, 29 Nov - 3 Dec 2021

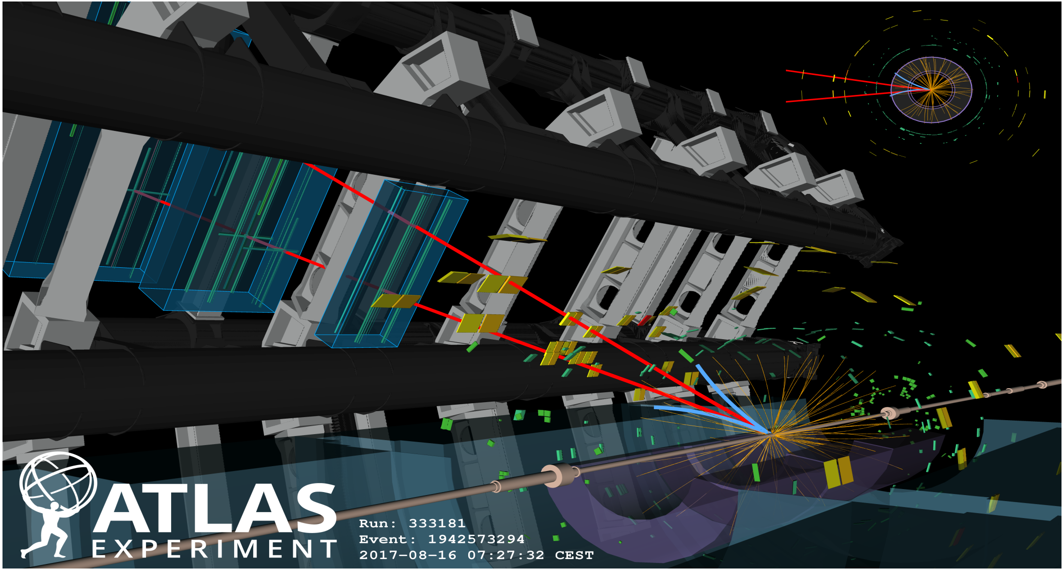
ATLAS
EXPERIMENT
Run: 333181
Event: 1942573294
2017-08-16 07:27:32 CEST

Data taking conditions in ATLAS at p-p interactions at $\sqrt{s}$ = 13 TeV

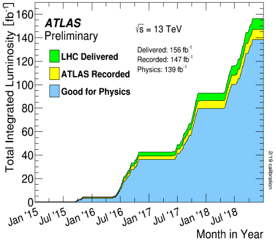

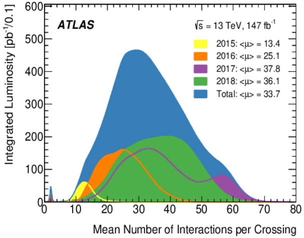

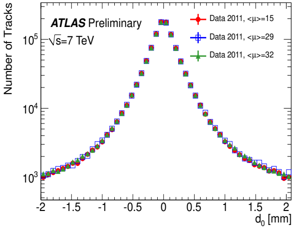

- ATLAS collected 147 fb^{-1} of 156 fb^{-1} of the luminosity delivered by LHC in Run2, with 136 fb^{-1} for physics, Fig left
- Nº of interactions per crossing up to 70, with mean values between 13-38 in years - Fig middle
- To benefit from high integrated luminosity ATLAS B-physics must pay attention to
  - Specialised B-triggers - to maintain increasing event rates
  - Stability of tracking and vertexing performance at high pileups
  - Stability of track impact parameter resolution with increasing pileup, up to resolution tails - Fig right

ATLAS trigger strategy for B-physics analysis

- ATLAS has collected 139 fb^{-1} of data in Run 2, and 25 fb^{-1} in Run 1
- Focus mostly on final states with muons
- Typical triggers di-muons with p_{T} thresholds of either 4 GeV or 6 GeV (vary over run periods)
- Additional trigger selections are applied, e.g. on di-muon masses, targeting different analysis, as shown in Fig below

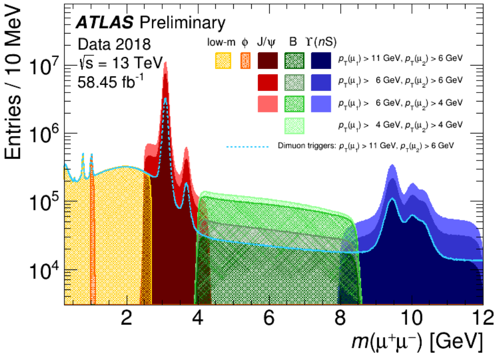

ATLAS detector

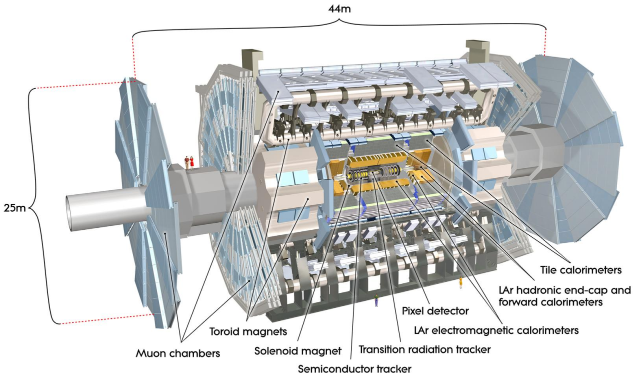

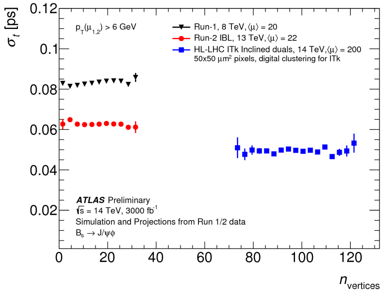

Time resolution of $B_s^0 \to J/\psi\phi$ for different numbers of reconstructed PV in the same bunch crossing.

- Inner Detector: PIX, SCT and TRT, $p_{\mathrm{T}} > 0.4\,\mathrm{GeV}$, $|\eta| < 2.5$
  - Run2: new IBL 25% improvement of time resolution with respect to Run1
  - Time, mass resolutions remain stable within increasing pileup in Run 2
- Muon Spectrometer: triggering ($|\eta| < 2.4$), precision tracking ($|\eta| < 2.7$)

CP violation in $B_s^0 \to J/\psi(\mu^+\mu^-)\phi(K^+K^-)$

Motivation

- $B_s^0 \to J/\psi\phi$ is used to measure CP-violation phase ϕ_s potentially sensitive to New Physics (NP)
- In SM ϕ_s is related to the CKM elements $\phi_s \simeq 2\arg[-(V_{ts}V_{tb}^*)/(V_{cs}V_{cb}^*)]$ and predicted with high precision
  - $\phi_s = -0.03696^{+0.00072}_{-0.00082}$ rad by CKMFitter group PhysRevD.91.073007
  - $\phi_s = -0.03700 \pm 0.00104$ rad according to UTfit Collaboration arXiv: hep-ph/0606167 [hep-ph].
- LHC combined 2021: $\phi_s = -0.050 \pm 0.019$ rad, consistent with SM, however SM precision still 20 times better - room for New physics
- Other quantity related to B_s^0 mixing is $\Delta\Gamma_s = \Gamma_s^L - \Gamma_s^H$, Γ_s^L and Γ_s^H are the decay widths of the mass eigenstates. $\Delta\Gamma_s$ was calculated in SM arXiv:1912.07621v2 [hep-ph] and new experimental results needed to tighten uncertainties and eventually get sensitivity to NP

ATLAS data in this analysis

- Results presented here use 80.5 fb^{-1} of 2015-17 data, combined with 19.2 fb^{-1} Run1
- Use $J/\psi \to \mu^+\mu^-$ triggers, with cuts on di-muon mass window. No low-limit cuts on L_{xy}, or on the impact parameter applied to avoid biasing B_s^0 proper-decay time
- Events selected for analysis contained $453\,570 \pm 740$ $B_s^0 \to J/\psi\phi$ signals

Inclusion of angular analysis - necessary part of extraction of the CP violation phase ϕ_s

- $B_s^0 \to J/\psi\phi$ = pseudoscalar to vector-vector
- Final state: admixture of CP-odd ($L = 1$) and CP-even ($L = 0, 2$) states
- Distinguishable through time-dependent angular analysis
- Non-resonant S-wave decay $B_s^0 \to J/\psi K^+ K^-$ contribute to the final state
- Included in the differential decay rate due to interference with the $B_s^0 \to J/\psi(\mu^+\mu^-)\psi(K^+K^-)$ decay

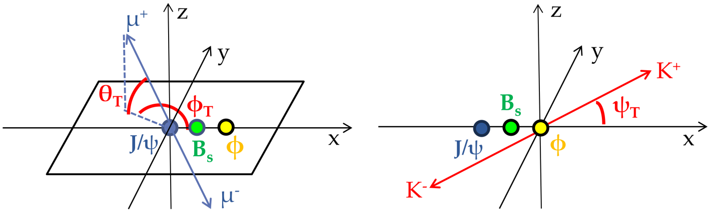

Figure: Angles between final state particles in transversity basis.

Mass-lifetime-angular fit

We perform unbinned maximum likelihood fit simultaneously for B_s^0 mass, decay time and the decay angles:

$$\begin{aligned}\ln\ \mathcal{L} = \sum_{i=1}^{N}\{ & w_i \cdot \ln(f_{\rm s} \cdot \mathcal{F}_{\rm s}(m_i, t_i, \sigma_m, \sigma_t, \Omega_i, P(B|Q), p_{\mathrm{T}_i}) \\ & + f_{\rm s} \cdot f_{B_d^0} \cdot \mathcal{F}_{B_d^0}(m_i, t_i, \sigma_m, \sigma_t, \Omega_i, P(B|Q), p_{\mathrm{T}_i}) \\ & + f_{\rm s} \cdot f_{\Lambda_b} \cdot \mathcal{F}_{\Lambda_b}(m_i, t_i, \sigma_m, \sigma_t, \Omega_i, P(B|Q), p_{\mathrm{T}_i}) \\ & + (1 - f_{\rm s} \cdot (1 + f_{B_d^0} + f_{\Lambda_b})) \cdot \mathcal{F}_{\rm bkg}(m_i, t_i, \sigma_m, \sigma_t, \Omega_i, P(B|Q), p_{\mathrm{T}_i}))\}\end{aligned}$$

Physics parameters

- CPV phase ϕ_s
- Decay widths: $\Delta\Gamma_s$, Γ_s
- Decay amplitudes: $|A_0(0)|^2$, $|A_{||}(0)|^2$, $\delta_{||}$, $\delta_{\perp}$
- S-wave: $|A_S(0)|^2$, δ_S
- Δm_s fixed to PDG
- Assuming no direct CPV, the amplitude λ related to ϕ_s as $\phi_s = -\arg\lambda$ fixed to 1

Observables

- Basic observables : m_i, t_i, Ω_i
- Conditional observables per-candidate:
  - resolutions: σ_{m_i}, σ_{t_i}
  - tagging probability and method: $P(B|Q)$

Flavour tagging

- Opposite side tagging
- Use Muon or Electron
  - $b \to l$ transitions are clean tagging method
  - $b \to c \to l$ and neutral B-meson oscillations dilute the tagging
- Jet-Charge
  - information from tracks in b-tagged jet, when no lepton is found
- Calibration using $B^{\pm} \to J/\psi K^{\pm}$ data

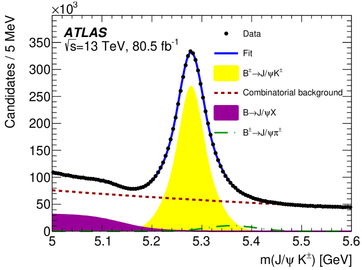

Inv. mass $B^{\pm} \to J/\psi K^{\pm}$. Data shown as points, overall fit result blue curve, other curves signal and background fits.

Tag method	ϵ_x [%]	D_x [%]	T_x [%]
Tight muon	4.50 ± 0.01	43.8 ± 0.2	0.862 ± 0.009
Electron	1.57 ± 0.01	41.8 ± 0.2	0.274 ± 0.004
Low-p_T muon	3.12 ± 0.01	29.9 ± 0.2	0.278 ± 0.006
Jet	12.04 ± 0.02	16.6 ± 0.1	0.334 ± 0.006
Total	21.23 ± 0.03	28.7 ± 0.1	1.75 ± 0.01

Efficiency: $\varepsilon = \frac{N_{\text{tagged}}}{N_{\text{Bcand}}}$, Dilution: $D = (1 - 2w)$, w miss-tag probability, Tagging Power: $TP = \varepsilon D^2$

Results 2015-2017 data: Projections of the mass-lifetime-angular fit

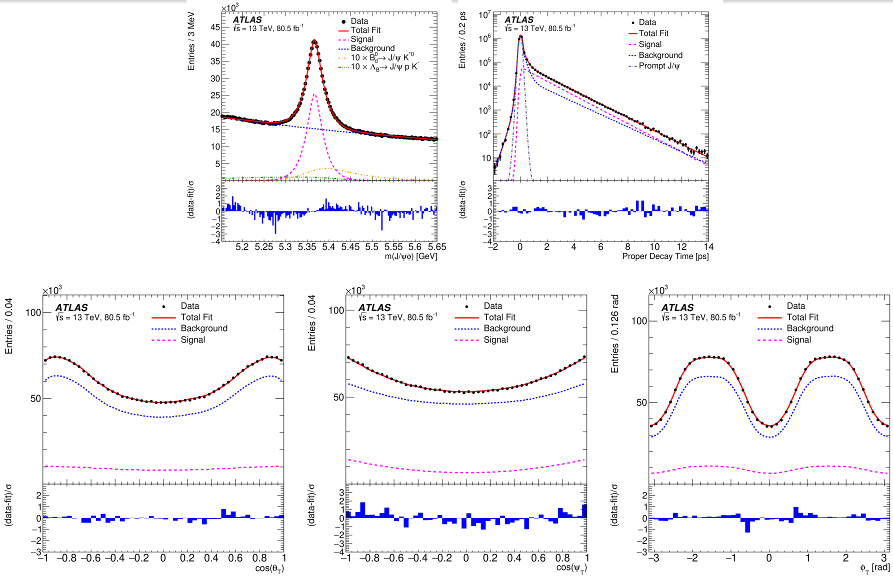

Results 2015-2017 data: fit parameters

- While for most of the physics parameters, including ϕ_s , $\Delta\Gamma_s$, Γ_s, the fit determines a single solution, for the strong-phases $\delta_{||}$ and $\delta_{\perp}$ two well separated local maxima of the likelihood are found, and shown as solution (a) and (b) in table of results
- The difference in likelihoods, $-2\Delta\ln(L)$, between the two solutions is equal to 0.03, favouring (a) but without ruling out (b)

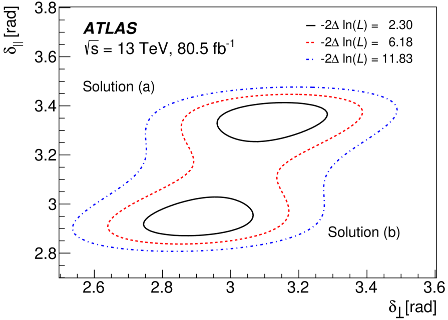

Parameter	Value	Statistical uncertainty	Systematic uncertainty
ϕ_s [rad]	−0.081	0.041	0.022
$\Delta\Gamma_s$ [ps^{-1}]	0.0607	0.0047	0.0043
Γ_s [ps^{-1}]	0.6687	0.0015	0.0022
$\lvert A_{\parallel}(0)\rvert^2$	0.2213	0.0019	0.0023
$\lvert A_0(0)\rvert^2$	0.5131	0.0013	0.0038
$\lvert A_S(0)\rvert^2$	0.0321	0.0033	0.0046
$\delta_\perp - \delta_S$ [rad]	−0.25	0.05	0.04
Solution (a)			
$\delta_\perp$ [rad]	3.12	0.11	0.06
$\delta_\parallel$ [rad]	3.35	0.05	0.09
Solution (b)			
$\delta_\perp$ [rad]	2.91	0.11	0.06
$\delta_\parallel$ [rad]	2.94	0.05	0.09

ATLAS $B_s^0 \to J/\psi\phi$ Combination Run2 + 1. Comparison with CMS and LHCb

Parameter	Solution (a) Value	Statistical uncertainty	Systematic uncertainty
ϕ_s [rad]	−0.087	0.036	0.021
$\Delta\Gamma_s$ [ps^{-1}]	0.0657	0.0043	0.0037
Γ_s [ps^{-1}]	0.6703	0.0014	0.0018
$\lvert A_\parallel(0)\rvert^2$	0.2220	0.0017	0.0021
$\lvert A_0(0)\rvert^2$	0.5152	0.0012	0.0034
$\lvert A_S\rvert^2$	0.0343	0.0031	0.0045
$\delta_\perp$ [rad]	3.22	0.10	0.05
$\delta_\parallel$ [rad]	3.36	0.05	0.09
$\delta_\perp - \delta_S$ [rad]	−0.24	0.05	0.04

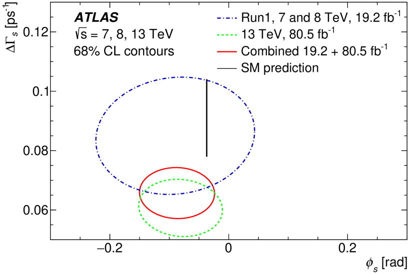

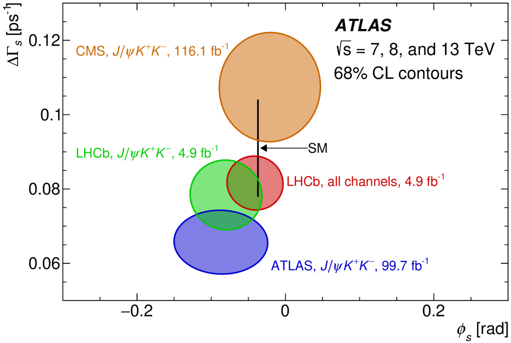

- ϕ_s result consistent with results from CMS, LHCb and SM
- Competitive single measurement of $\Delta\Gamma_s$, Γ_s and helicity parameters
- Still to add 60 fb^{-1} from 2018

- Increase $>$ 10 x $\int$ Ldt of LHC $\to$ 3000-4000 fb^{-1}
- Peak luminosity 5 - 7.5 x 10^{34} cm^{-2} s^{-1}
- Average amount of pp interactions 140-200 per BX with a time space 25 ns
- These conditions require Detector Upgrades

High Luminosity-LHC - ATLAS track density in Inner detector

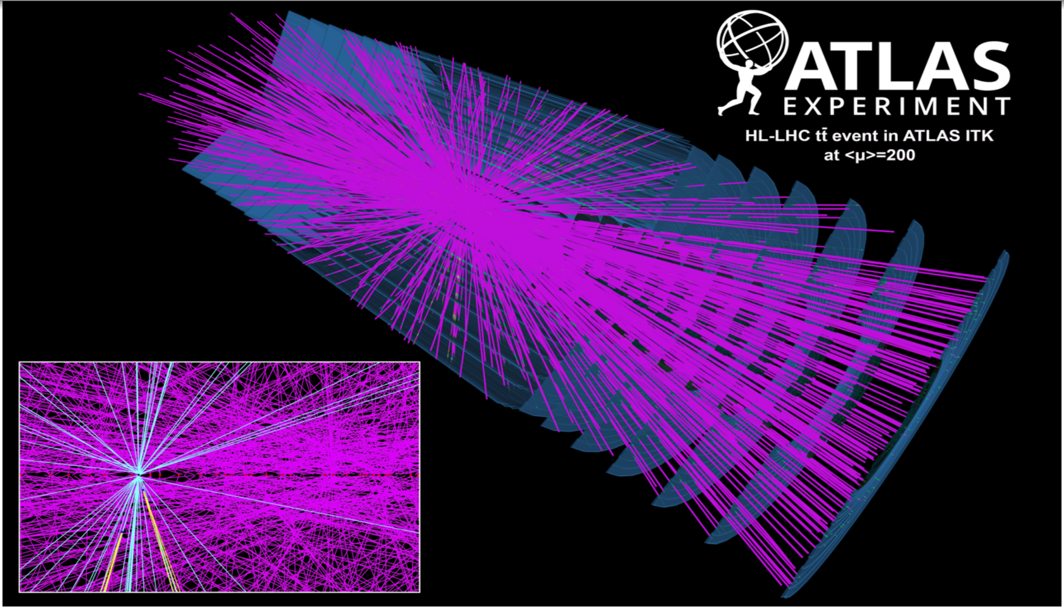

New all-silicon detector

- ITk pixel (13 m^2)
  - 5 barrel, 5 EC layers (with rings)
  - Inclined sensors
  - Extends to η = 4.0 (2.5 now)
  - Innermost layer at 36 mm
  - 580 M channels (80 M now)
- ITk strips (160 m^2)
  - 4 barrel layers, 6 EC rings
  - 50 M channels (6 M now)
  - Strip occupancy $<$1%
- Material considerably reduced

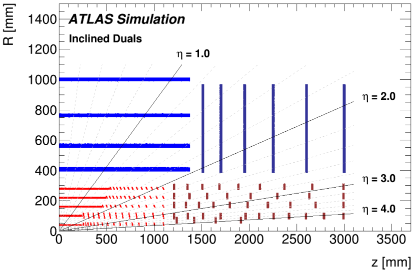

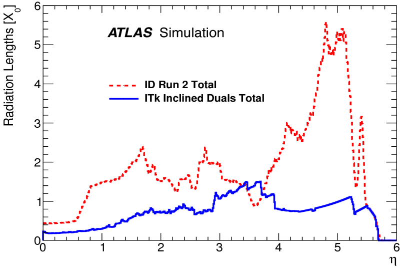

ATL-PHYS-PUB-2018-041

- ID upgrade: proper decay time resolution improved by 18% w.r.t. Run 2 and still stable at 200 collisions/BX
- Three trigger scenarios for muon momenta thresholds
- ϕ_s precision improves (9 - 20) times w.r.t.Run1, or (4 - 9) times w.r.t. current result combining Run1 and Run2 99.7 fb^{-1}

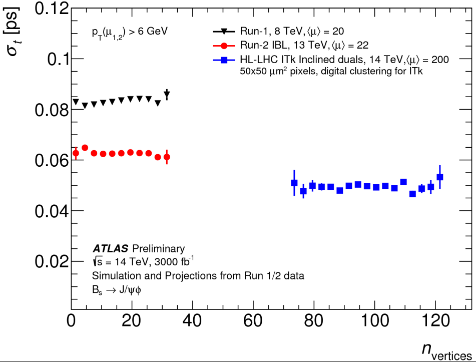

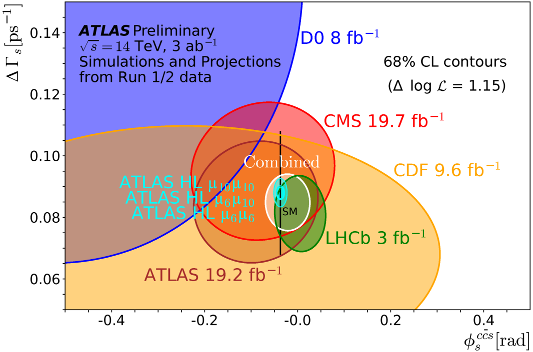

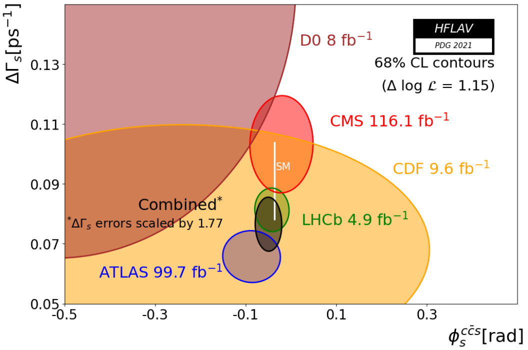

Case of CP violation phase ϕ_s

- In SM ϕ_s is related to the CKM elements $\phi_s \simeq 2\arg[-(V_{ts}V_{tb}^*)/(V_{cs}V_{cb}^*)]$ and predicted with high precision
  - $\phi_s = -0.03696^{+0.00072}_{-0.00082}$ rad by CKMFitter group PhysRevD.91.073007
  - $\phi_s = -0.03700 \pm 0.00104$ rad according to UTfit Collaboration arXiv: hep-ph/0606167 [hep-ph].
- LHC combined 2021: $\phi_s = -0.050 \pm 0.019$ rad, consistent with SM. All experiments consistent with each other and with SM
- SM precision still 20 times better - there is a room for New physics
- An answer is on experimental side: Run3 LHC and HL-LHC needed to tighten experimental uncertainties

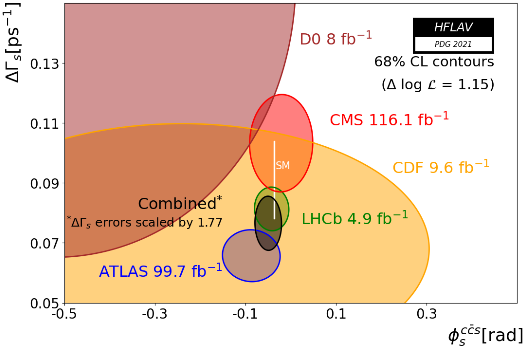

Case of $\Delta\Gamma_s$

- SM calculations:
  - $\Delta\Gamma_s = 0.091 \pm 0.013$ ps-1 Lenz et.al
- A potential NP enhancement of ϕ_s would also decrease $\Delta\Gamma_s$, but not as significantly Lenz1
- Experiments consistent with SM within $<1.3\ \sigma$
- Some tensions between CMS and ATLAS at level of 2 σ, still more Run2 data to analyse

Summary

- ATLAS analysis of $B_s^0 \to J/\psi\phi$ combining Run1 and Run2 99.7 fb^{-1} show the CP violation phase ϕ_s compatible with SM
- ATLAS continues with including 2018 data and is ready for Run3 data taking, to increase precision on ϕ_s and other variables of interest: $\Delta\Gamma_s$, Γ_s
- At HL-LHC with upgraded ATLAS detector the ϕ_s precision will improve by (4 - 9) times w.r.t. Run2
- Current World combination of ϕ_s is consistent with SM, while there is evidently room for New Physics contributions
- All LHC experiments are prepared to continue this research with Run3 and HL-LHC

Backup Slides

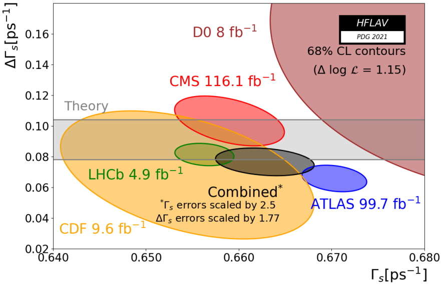

Because of tensions between the measurements, the errors on Γ_s and $\Delta\Gamma_s$ have been scaled by 2.5 and 1.77, respectively (the ellipses representing the results of each experiment are shown before scaling, while the combined ellipses include the scale factors).

Case of $\Delta\Gamma_s$

- SM calculations:
  - $\Delta\Gamma_s = 0.091 \pm 0.013$ ps-1 Lenz et.al
- A potential NP enhancement of ϕ_s would also decrease $\Delta\Gamma_s$, but not as significantly Lenz1
- Experiments consistent with SM within $<1.3\ \sigma$
- Some tensions between CMS and ATLAS at level of 2 σ, still more Run2 data to analyse

Case of Γ_s

- Currently tensions in measurements of Γ_s, more Run2 data to analyse
- SM paper Kirk et.al 2020 do not expect NP effects
- Recent note admits that precise experimental knowledge on B-lifetimes Ratios, can provide bounds on NP models LenzOct2021
- ATLAS: to use full Run2 data to bring more results on lifetimes

Full likelihood function

k	$O^{(k)}(t)$	$g^{(k)}(\theta_T,\psi_T,\phi_T)$
1	$\frac{1}{2}\lvert A_0(0)\rvert^2\left[(1+\cos\phi_s)\,e^{-\Gamma_{\rm L}^{(s)}t}+(1-\cos\phi_s)\,e^{-\Gamma_{\rm H}^{(s)}t}\pm 2e^{-\Gamma_s t}\sin(\Delta m_s t)\sin\phi_s\right]$	$2\cos^2\psi_T(1-\sin^2\theta_T\cos^2\phi_T)$
2	$\frac{1}{2}\lvert A_\parallel(0)\rvert^2\left[(1+\cos\phi_s)\,e^{-\Gamma_{\rm L}^{(s)}t}+(1-\cos\phi_s)\,e^{-\Gamma_{\rm H}^{(s)}t}\pm 2e^{-\Gamma_s t}\sin(\Delta m_s t)\sin\phi_s\right]$	$\sin^2\psi_T(1-\sin^2\theta_T\sin^2\phi_T)$
3	$\frac{1}{2}\lvert A_\perp(0)\rvert^2\left[(1-\cos\phi_s)\,e^{-\Gamma_{\rm L}^{(s)}t}+(1+\cos\phi_s)\,e^{-\Gamma_{\rm H}^{(s)}t}\mp 2e^{-\Gamma_s t}\sin(\Delta m_s t)\sin\phi_s\right]$	$\sin^2\psi_T\sin^2\theta_T$
4	$\frac{1}{2}\lvert A_0(0)\rvert\lvert A_\parallel(0)\rvert\cos\delta_\parallel$ $\left[(1+\cos\phi_s)\,e^{-\Gamma_{\rm L}^{(s)}t}+(1-\cos\phi_s)\,e^{-\Gamma_{\rm H}^{(s)}t}\pm 2e^{-\Gamma_s t}\sin(\Delta m_s t)\sin\phi_s\right]$	$\frac{1}{\sqrt{2}}\sin 2\psi_T\sin^2\theta_T\sin 2\phi_T$
5	$\lvert A_\parallel(0)\rvert\lvert A_\perp(0)\rvert[\frac{1}{2}(e^{-\Gamma_{\rm L}^{(s)}t}-e^{-\Gamma_{\rm H}^{(s)}t})\cos(\delta_\perp-\delta_\parallel)\sin\phi_s$ $\pm e^{-\Gamma_s t}(\sin(\delta_\perp-\delta_\parallel)\cos(\Delta m_s t)-\cos(\delta_\perp-\delta_\parallel)\cos\phi_s\sin(\Delta m_s t))]$	$-\sin^2\psi_T\sin 2\theta_T\sin\phi_T$
6	$\lvert A_0(0)\rvert\lvert A_\perp(0)\rvert[\frac{1}{2}(e^{-\Gamma_{\rm L}^{(s)}t}-e^{-\Gamma_{\rm H}^{(s)}t})\cos\delta_\perp\sin\phi_s$ $\pm e^{-\Gamma_s t}(\sin\delta_\perp\cos(\Delta m_s t)-\cos\delta_\perp\cos\phi_s\sin(\Delta m_s t))]$	$\frac{1}{\sqrt{2}}\sin 2\psi_T\sin 2\theta_T\cos\phi_T$
7	$\frac{1}{2}\lvert A_S(0)\rvert^2\left[(1-\cos\phi_s)\,e^{-\Gamma_{\rm L}^{(s)}t}+(1+\cos\phi_s)\,e^{-\Gamma_{\rm H}^{(s)}t}\mp 2e^{-\Gamma_s t}\sin(\Delta m_s t)\sin\phi_s\right]$	$\frac{2}{3}\left(1-\sin^2\theta_T\cos^2\phi_T\right)$
8	$\alpha\lvert A_S(0)\rvert\lvert A_\parallel(0)\rvert[\frac{1}{2}(e^{-\Gamma_{\rm L}^{(s)}t}-e^{-\Gamma_{\rm H}^{(s)}t})\sin(\delta_\parallel-\delta_S)\sin\phi_s$ $\pm e^{-\Gamma_s t}(\cos(\delta_\parallel-\delta_S)\cos(\Delta m_s t)-\sin(\delta_\parallel-\delta_S)\cos\phi_s\sin(\Delta m_s t))]$	$\frac{1}{3}\sqrt{6}\sin\psi_T\sin^2\theta_T\sin 2\phi_T$
9	$\frac{1}{2}\alpha\lvert A_S(0)\rvert\lvert A_\perp(0)\rvert\sin(\delta_\perp-\delta_S)$ $\left[(1-\cos\phi_s)\,e^{-\Gamma_{\rm L}^{(s)}t}+(1+\cos\phi_s)\,e^{-\Gamma_{\rm H}^{(s)}t}\mp 2e^{-\Gamma_s t}\sin(\Delta m_s t)\sin\phi_s\right]$	$\frac{1}{3}\sqrt{6}\sin\psi_T\sin 2\theta_T\cos\phi_T$
10	$\alpha\lvert A_0(0)\rvert\lvert A_S(0)\rvert[\frac{1}{2}(e^{-\Gamma_{\rm H}^{(s)}t}-e^{-\Gamma_{\rm L}^{(s)}t})\sin\delta_S\sin\phi_s$ $\pm e^{-\Gamma_s t}(\cos\delta_S\cos(\Delta m_s t)+\sin\delta_S\cos\phi_s\sin(\Delta m_s t))]$	$\frac{4}{3}\sqrt{3}\cos\psi_T\left(1-\sin^2\theta_T\cos^2\phi_T\right)$

$$\ln \mathcal{L} = \sum_{i=1}^{N} \{ \underbrace{w_i}_{\text{Tau weight}} \cdot \ln(\underbrace{f_s \cdot \mathcal{F}_s}_{\text{Signal}} + \underbrace{f_s \cdot f_{B_d^0} \cdot \mathcal{F}_{B_d^0} + f_s \cdot f_{\Lambda_b} \cdot \mathcal{F}_{\Lambda_b}}_{\text{Peaking background}} + \underbrace{(1 - f_s \cdot (1 + f_{B_d^0} + f_{\Lambda_b})) \cdot \mathcal{F}_{\text{bkg}}}_{\text{Combinatorial background}})\}$$

- Data are corrected by the decay time correction
- Mass as well as lifetime use per-candidate width and scale factor, with flavour-dependent terms weighted by tagging probability $P(B|Q)$
- Contributions from $B_d^0 \to J/\psi K^{*0}$, $B_d^0 \to J/\psi K\pi$ and $\Lambda_b^0 \to J/\psi Kp$ due to wrong mass assignment (KK)
  - Efficiencies and acceptance from MC
  - BR from PDG
  - Fragmentation fractions from other measurements
- Combinatorial background for angular distribution use Legendre polynomials from sidebands; fixed in the main fit

Systematic uncertainties

- Systematics assumed uncorrelated $\rightarrow$ Total = $\sqrt{\sum_i \text{syst}_i^2}$
- Tagging systematics dominant for ϕ_s
  - Accounting for pile-up dependence, calibration curves model and MC precision, ”Punzi” PDFs variations, difference between $B^{\pm}$ and B_s^0 kinematics
- Fit-model time resolution systematics dominant for Γ_s and $\Delta\Gamma_s$

	ϕ_s [rad]	$\Delta\Gamma_s$ [ps^{-1}]	Γ_s [ps^{-1}]	$\lvert A_{\parallel}(0)\rvert^2$	$\lvert A_0(0)\rvert^2$	$\lvert A_S(0)\rvert^2$	$\delta_{\perp}$ [rad]	$\delta_{\parallel}$ [rad]	$\delta_{\perp}-\delta_S$ [rad]
Tagging	1.7×10^{-2}	0.4×10^{-3}	0.3×10^{-3}	0.2×10^{-3}	0.2×10^{-3}	2.3×10^{-3}	1.9×10^{-2}	2.2×10^{-2}	2.2×10^{-3}
Acceptance	0.7×10^{-3}	$<10^{-4}$	$<10^{-4}$	0.8×10^{-3}	0.7×10^{-3}	2.4×10^{-3}	3.3×10^{-2}	1.4×10^{-2}	2.6×10^{-3}
ID alignment	0.7×10^{-3}	0.1×10^{-3}	0.5×10^{-3}	$<10^{-4}$	$<10^{-4}$	$<10^{-4}$	1.0×10^{-2}	7.2×10^{-3}	$<10^{-4}$
S–wave phase	0.2×10^{-3}	$<10^{-4}$	$<10^{-4}$	0.3×10^{-3}	$<10^{-4}$	0.3×10^{-3}	1.1×10^{-2}	2.1×10^{-2}	8.3×10^{-3}
Background angles model:									
Choice of fit function	1.8×10^{-3}	0.8×10^{-3}	$<10^{-4}$	1.4×10^{-3}	0.7×10^{-3}	0.2×10^{-3}	8.5×10^{-2}	1.9×10^{-1}	1.8×10^{-3}
Choice of p_{T} bins	1.3×10^{-3}	0.5×10^{-3}	$<10^{-4}$	0.4×10^{-3}	0.5×10^{-3}	1.2×10^{-3}	1.5×10^{-3}	7.2×10^{-3}	1.0×10^{-3}
Choice of mass interval	0.4×10^{-3}	0.1×10^{-3}	0.1×10^{-3}	0.3×10^{-3}	0.3×10^{-3}	1.3×10^{-3}	4.4×10^{-3}	7.4×10^{-3}	2.3×10^{-3}
Dedicated backgrounds:									
B_d^0	2.3×10^{-3}	1.1×10^{-3}	$<10^{-4}$	0.2×10^{-3}	3.1×10^{-3}	1.4×10^{-3}	1.0×10^{-2}	2.3×10^{-2}	2.1×10^{-3}
Λ_b	1.6×10^{-3}	0.4×10^{-3}	0.2×10^{-3}	0.5×10^{-3}	1.2×10^{-3}	1.8×10^{-3}	1.4×10^{-2}	2.9×10^{-2}	0.8×10^{-3}
Fit model:									
Time res. sig frac	1.4×10^{-3}	1.1×10^{-3}	$<10^{-4}$	0.5×10^{-3}	0.6×10^{-3}	0.6×10^{-3}	1.2×10^{-2}	3.0×10^{-2}	0.4×10^{-3}
Time res. p_{T} bins	3.3×10^{-3}	1.4×10^{-3}	0.1×10^{-2}	$<10^{-4}$	$<10^{-4}$	0.5×10^{-3}	6.2×10^{-3}	5.2×10^{-3}	1.1×10^{-3}
Total	1.8×10^{-2}	0.2×10^{-2}	0.1×10^{-2}	0.2×10^{-2}	0.4×10^{-2}	0.4×10^{-2}	9.7×10^{-2}	2.0×10^{-1}	0.1×10^{-1}